SAND2011-0404C

Die/wafer Sub-micron Alignment Strategies for Semiconductor Device Integration

Lauren E. Shea-Rohwer, James E. Martin, Dahwey Chu

Sandia National Laboratories, P.O. Box 5800, MS0892, Albuquerque, New Mexico 87185, USA

This study explores self-aligning patterns to achieve sub-micron alignment of die/wafers. We have patterned 2-d arrays of gold lines, whose width is half the periodicity, onto substrates. When commensurate patterns are brought into contact, the surface interactions between the Au lines enables high-resolution alignment, manually. Self-assembled monolayers of alkanethiols on the Au, further enhance the surface interactions, enabling alignment in less than half the time as for the uncoated die. A computation of the alignment force and torque between two featured surfaces illustrates how best to pattern surfaces to maximize the tendency to align. An array of lines with a sinusoidal modulation in their spacing is more tolerant of initial misalignment, yet retains the high registration force of periodic line arrays. The optimal registration pattern might be a single spiral, as it generates both a radial force and a torque. Such patterns on die/wafers would enable precision device integration.

Introduction

Background

It is currently only possible to align micropatterned features on die and wafers with those on other die and wafers with an accuracy of no better than ~5 microns, using the highest precision alignment equipment. To enable the integration of devices with ever-smaller feature sizes and increasing interconnect densities, sub-micron alignment is required.

Previous work on die/wafer alignment employs capillary force-assisted alignment techniques (1-6). Srinivasan *et al*. (1) used this approach to assemble microdevices patterned with square gold pads onto substrates with matching square gold pads, with an alignment accuracy of <0.2 μm. The Au pads on the microdevices and substrates are made hydrophobic with self-assembled monolayers (SAMs) of alkanethiols and an adhesive, respectively. The substrate is placed in a beaker of water and the microdevices are immersed in the water and directed to the substrate surface with a pipette. When the complementary hydrophobic patterns come into contact, the interfacial energy minimization of the adhesive-water and SAM-water interfaces leads to shape matching. The microdevices are held in place under water by the capillary forces of the adhesive, then permanently bonded by curing the adhesive with UV light (for transparent substrates) or heat (for opaque substrates).

There has been some effort to develop a capillary-force-assisted alignment approach that does not involve adhesives (2,4). Water droplets that are confined within hydrophilic "cells" having hydrophobic gold borders have been used to align 2-in. to 3-in. wafers (2). When wafers having complementary hydrophilic/hydrophobic cells are pressed together, alignment is driven by the capillary forces of the water droplets. This method achieved an alignment accuracy of <1 μm, but the water trapped between the wafers is problematic for permanent bonding and for sensitive devices.

Passive wafer alignment methods are promising alternatives to capillary force-assisted methods. In Ref. 7, silicon wafers were KOH-etched with mating features (pyramids, v-trenches), enabling an

alignment accuracy of 1 μm. Unfortunately, the etched surfaces are too rough for silicon direct and anodic bonding. A new approach to the problem of aligning, then bonding devices is clearly needed. In this work, we explore self-aligning patterns to achieve sub-micron alignment accuracy.

Technical Approach

Alignment force and torque

A computation of the alignment force and torque between two featured surfaces illustrates how best to pattern surfaces to maximize the tendency to align. We first consider the simple case of two surfaces patterned with lines, as in Figure 1. In this case there can be both a lateral and longitudinal force and a torque, and we will first compute the lateral force. Each surface is patterned with lines of width w with center-to-center separation d, and each line is of length L. The lines are comprised of material A, which in our experiments is Au that is sometimes coated with alkanethiols, and the gaps between the lines, of width (d-w), are material B, which we take as the underlying substrate, comprised of Pyrex or Si. The interfacial energies per unit area will be denoted as γ_{ij}, where i and j denote materials A or B. These are the actual energies of these surfaces brought into contact, including any effect of asperities and other imperfections.

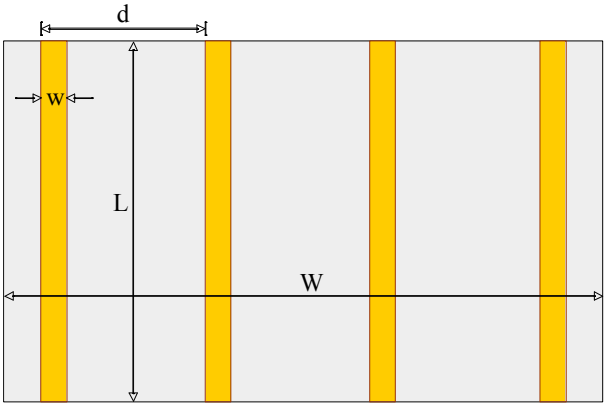

Figure 1. Patterning pattern intended to give alignment transverse to the lines.

Lateral force on an array of lines. In this case we assume the patterned lines are parallel and that the only misalignment is lateral to the lines, whose width $w \le d/2$. The variable x denotes the lateral displacement of the top surface relative to the bottom surface, which we take to be stationary, and $x=0$ corresponds to perfect alignment. For the case where $0 \le x \le w$, the interfacial energy per unit area of substrate is

$$\gamma = \frac{w-x}{d}\gamma_{\mathrm{AA}} + \frac{2x}{d}\gamma_{\mathrm{AB}} + \frac{d-w-x}{d}\gamma_{\mathrm{BB}}. \qquad [1]$$

Expressing the line width as $w=\alpha d$, where $\alpha \le 1/2$, gives

$$\gamma = \alpha\gamma_{AA} + (1-\alpha)\gamma_{BB} + \frac{x}{d}\Delta\gamma \qquad [2]$$

where the exchange energy per unit area is $\Delta\gamma = 2\gamma_{AB} - \gamma_{AA} - \gamma_{BB}$. The lateral *force per unit area f* is then just the negative spatial derivative of this areal energy,

$$f = -\frac{d\gamma}{dx} = -\Delta\gamma/d. \qquad [3]$$

For the lines to come into registration requires a negative force — which will occur for positive $\Delta\gamma$ — corresponding to those cases when materials A and B do not like to be in contact. Otherwise deregistration will be energetically favored. A plot of the surface energy and force are in Figure 2a. As a

rough estimate of the areal force we can take the exchange areal energy to be 10 ergs/cm^2. For a line spacing of 20 microns the areal force is then just 5x10^3 dynes/cm^2. For a 1 cm^2 substrate the lateral force would be roughly that due to earth's gravity on a 5 g mass, which is clearly palpable.

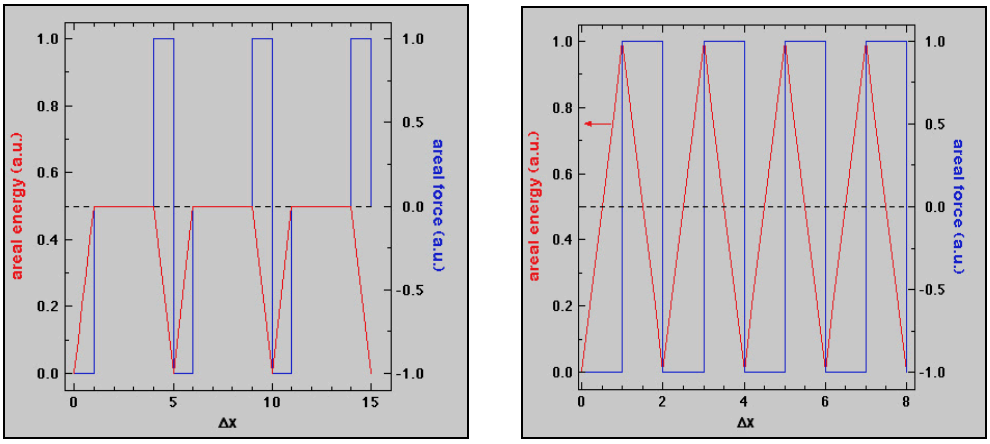

Figure 2. a) The registration surface energy and force as a function of lateral displacement. When there is no overlap between the material A lines (and therefore double overlap between the material B gaps between the lines) there is no force. b) In the case where the lines and spaces have the same width there are no force gaps of finite size.

A few aspects of Eq. 3 bear highlighting. First, the registration force is inversely proportional to the line spacing, but independent of the line width. Second, the areal force is an *intensive* property, being independent of the dimensions of the substrate, and because the areal static friction is also an intensive property, the ability of the registration force to overcome static friction is independent of scale. Third, in the case where the lines of material A do not partially overlap ($w<x<d-w$) the registration force will be zero. Avoiding this condition requires some care in the initial positioning of the top substrate, and this places an ultimate limitation of the periodicity of the lines. In the special case where the line width is just half the periodicity there is always a positive or negative force, Figure 2b, and this symmetric pattern gives the greatest tolerance of initial misregistration.

<u>*Longitudinal force on an array of lines*</u>. In this case the alignment force is due only to the edges of the substrate and is therefore extrinsic. For this reason we compute the *total* force F, not the areal force f. Let y denote the displacement parallel to the lines of the top substrate relative to the bottom substrate. The substrate is of size LxW, where L is the dimension parallel to the lines. The total surface energy Γ will be

$$\Gamma = (L-y)W\left[\frac{w}{d}\gamma_{AA} + \frac{d-w}{d}\gamma_{BB}\right] + 2yW\left[\frac{w}{d}\gamma_{A} + \frac{d-w}{d}\gamma_{B}\right] \qquad [4]$$

where γ_A and γ_B are the surface energies of materials A and B in contact with the surrounding atmosphere. Differentiating with respect to y gives the total force

$$F = W\left[\frac{w}{d}(2\gamma_A - \gamma_{AA}) + \frac{d-w}{d}(2\gamma_B - \gamma_{BB})\right] \qquad [5]$$

It is important to note that this total longitudinal force depends only on the substrate width and is *independent* of the size scale of the features. Furthermore, this force scales as W, whereas the static

friction scales as $L \times W$, so this longitudinal force is negligible in a practical sense. Substantial lateral and longitudinal forces require pad assemblies.

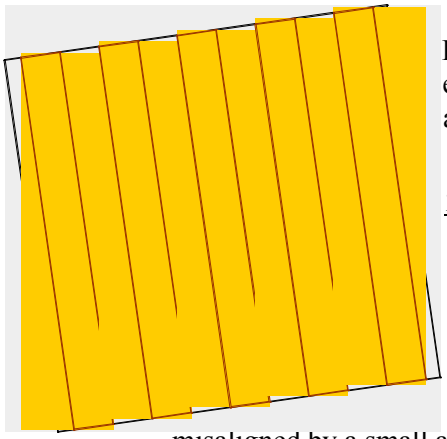

Figure 3. A series of lines misregistered by an angle □ that is small enough that the lines partially overlap throughout their length, creating a substantial alignment torque.

Torque on an array of lines. If there is angular misalignment between the substrates then an aligning torque can result. This torque will be zero if the angular misalignment is large enough that each line crosses several other lines, but can be quite substantial if the misalignment is so small that each line overlaps with the underlying line to some extent throughout its entire length, as illustrated in Figure 3. For a substrate of width W containing lines of length L misaligned by a small angle θ the surface energy is

$$\Gamma = \frac{W}{d}\frac{L^2}{2}\tan\theta\gamma_{AB} + \frac{W}{d}(wL - \frac{L^2}{4}\tan\theta)\gamma_{AA} + \frac{W}{d}\left((d-w)L - \frac{L^2}{4}\tan\theta\right)\gamma_{BB}$$
$$= \frac{W}{d}\left[wL\gamma_{AA} + (d-w)L\gamma_{BB} + \frac{L^2}{4}\Delta\gamma\tan\theta\right]. \qquad [6]$$

Differentiating this energy with respect to the angle θ gives the torque on the upper substrate

$$\mathrm{T} = -\frac{d\Gamma}{d\theta} \approx -A\frac{L}{4d}\Delta\gamma \qquad [7]$$

where the A is the substrate area. This expression is correct to order θ and shows that the torque is similar to the lateral force in that it increases with decreasing feature size d and so can be quite substantial. Of course, the torque also scales with the line length. In the simple case of a square substrate, where $L=W$, the registration torque scales as L^3, and the static friction in rotation also scales like L^3, so the ratio of the registration torque to the static friction is scale independent, and therefore of practical importance.

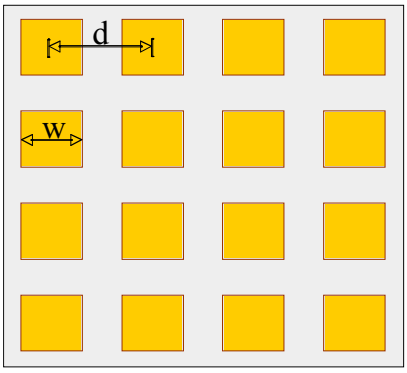

Figure 4. A square lattice of square pads.

Lateral and longitudinal force on a pad array. The lateral and longitudinal areal force on a square lattice of square pads of size w with lattice spacing d, Figure 4, is easily obtained from Eq. 3. The pad array can be viewed as a series of dashed lines, so the lateral force is simply reduced from the expression in Eq. 3 by the factor w/d. The longitudinal areal force is clearly equal to this lateral areal force,

$$f = \frac{w}{d^2}\Delta\gamma \qquad [8]$$

For the reasonable case where $w = \frac{1}{2}d$ this areal force is just one half that obtained with lines.

More complex registration patterns. The periodic patterns we have analyzed above have the fault that the surface energy has many strong local minima (see Figure 2). Thus it is possible to have registration errors at integer multiples of the lattice periodicity. Simply increasing the line width is not a good approach, as the width of the potential wells scales with the line spacing, causing the registration force to decrease with increasing line width. It is better to create a pattern that maintains both the depth and width of the registration well of a fine line pattern, yet somehow increases the spacing between wells. To eliminate this problem one could use various sorts of patterns that lack translational symmetry or have translational symmetry on a length scale large compared to the placement accuracy, and perhaps substantially larger than the line spacing. To illustrate this concept we consider the simple example of an array of lines with a sinusoidal modulation in their spacing.

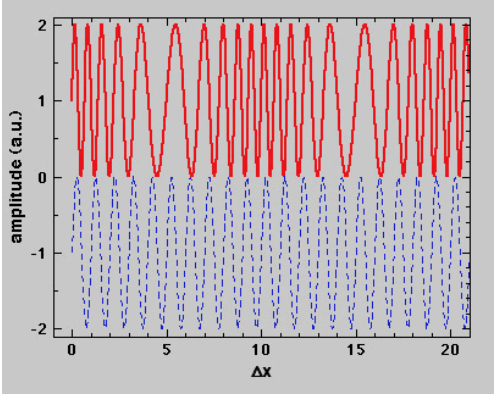

Figure 5. A phase-modulated surface composition fluctuation (solid line) is shown above a simple sinusoidal composition fluctuation with the same number of oscillations per unit length. The phase-modulated function has ten times the unit cell.

To simplify the computation of the interaction energy we consider a mathematical model that captures the *spirit* of this approach: a continuous composition modulation of the form $C(x) = \sin(2\pi kx + \phi(x))$, where $\phi(x) = A\sin(2\pi k' x)$. The 'potential surface' is then defined by the integral $U(\Delta x) = -\lim_{X\to\infty}\frac{1}{X}\int_0^X C(x)C(x+\Delta x)dx$. In Figure 5 we compare the unmodulated pattern (k=1, A=0) with the modulated pattern having k=1, k'=0.1, and A=5. In Figure 6 we give the potential surfaces for these two cases. The phase-modulated function increases the periodicity of the potential by a factor of k/k'=10, and decreases the amplitude of the minima in between the principal minima. Further increases in k/k' will increase the periodicity and greatly decrease the magnitude of the potential surface between the principal minima. This approach could greatly reduce the need for precision placement, while still retaining the high registration force given by fine lines. If this modulation had a periodicity of ten lines, then the initial registration accuracy could be reduced by a factor of ten without fear of misregistraion. Alignment parallel to the lines could be achieved simply by making the lines wavy. These waves could also be phase modulated.

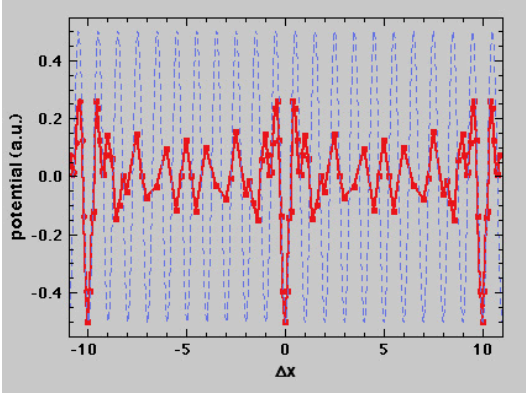

Figure 6. A comparison between the potential surfaces of the simple sinusoidal (dashed line) and phase-modulated composition fluctuations. If the phase-modulation wavevector is increased, the potential in between the principal minima is greatly reduced.

Many other approaches are possible. For example, Figure 7 shows the Moire pattern that occurs when two patterns of regularly spaced rings overlap. The surface

energy is a weak function of the separation of the centers of these two patterns, until they come very close to concentricity. So one would expect a *single strong energy minimum*, and an associated radial force, to occur whose size is on the scale of the ring diameter, eliminating the possibility of misregistration. Of course, such a pattern would not generate a torque, but if two such patterns were on opposing corners of a die a large torque would occur. On the other hand, a single spiral pattern would generate both a radial force with a single minimum *and* a torque with a single minimum. Perhaps that is the optimal registration pattern.

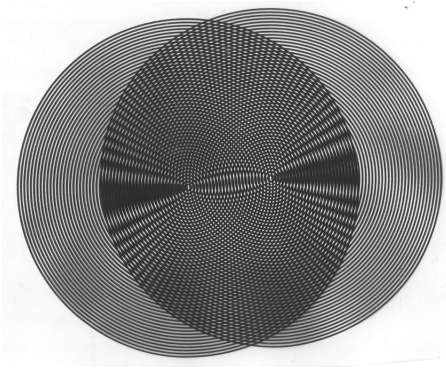

Figure 7. Moire pattern between two patterns of regular spaced rings.

<u>*Comments about the surface energies*</u>. In the analysis above we have modeled the surface interactions as if the patterned substrates are perfectly planarized. This is not the case in our experiments, where the Au lines are patterned onto a Pyrex substrate. These lines are 220 nm thick (including the Cr adhesion layer), and thus the Pyrex never comes into contact with either the Pyrex or Au on the opposing substrate. The interfacial energies in the exchange energy must be modified to reflect that gaps exist and that the Pyrex surfaces are actually in contact with the atmosphere. Letting the subscript A refer to Au, the interfacial energy γ_{AB} becomes $\gamma_A + \gamma_B$ the interfacial energy γ_{BB} becomes $2\gamma_B$, and the exchange energy becomes $\Delta\gamma = 2\gamma_A - \gamma_{AA}$. So the registration force is solely due to the Au interactions, or to the interactions of the ligands on the Au surfaces, as the case may be. In addition, if the Au features are rough then their surfaces will only be in partial contact, which will further reduce the observed exchange energy.

Experimental Procedure

<u>Alignment experiments</u>

Our test pattern is an array of lines photolithograhically deposited onto Pyrex wafers. Each die is 2 cm square with 25 μm Au lines separated by 25 μm. The Au lines are 200 nm thick deposited onto a 20 nm thick chromium adhesion layer. The Au lines were left bare, or were coated with dodecanethiol. Before they were coated, the substrates were cleaned in a 5:1:1 solution of deionized water, H_2SO_4, and 30% H_2O_2 for 5 min., rinsed in water, air dried, then immersed in a 1mM solution of dodecanethiol in ethanol for 24 h., rinsed in ethanol, and air dried.

<u>Bonding experiments</u>

We evaluated the shear strength of Au-Au bonds as a function of the Au surface treatment. Our experiments used ~1 cm square silicon die with either an 8x8 array of Au stud bumps; or 24x40 arrays of electroless nickel, immersion gold (ENIG) or electroless nickel, electroless palladium, immersion gold (ENEPIG) pads. The 8x8 arrays were made by wire bonding 25 μm Au wire to 100 μm square gold pads. The ENIG/ENEPIG arrays were fabricated at PacTech and consist of 1 μm thick aluminum-1% silicon pads with 5, 10, or 25 μm thick Ni, 0.35 μm of Pd, and 100 nm of Au. The pads are ~80 μm diameter on 400 μm spacings.

The arrays were either coated with dodecanethiol using the method described previously, or were Argon plasma cleaned for 5 min. (375W, 15 psi). The bonds were made using a Finetech Lambda at 150-

155°C for 30-45 seconds under 20N of force; and 185°C for 30 minutes under 200N of force for the stud bump and the ENIG/ENEPIG arrays, respectively. The bonds were sheared using a Dage 4000 shear tester.

Results and Discussion

Experimental validation of registration

In this section we present the results of the experiments that were conducted to demonstrate that patterned features can lead to high resolution registration, in fact, far better than can be produced by our aligner. Our first experiments utilized 2 cm square Pyrex substrates patterned with 25 μm Au lines, as described previously. Only the Au lines on opposing die can come into contact, unless the two die come together out of registration, which did not occur.

One die was placed on a microscope stage and the second die was placed on top, which generally produced a Moire pattern indicative of a relative misorientation, as in Figure 8.

Figure 8. Moire pattern between two identical sets of equally spaced lines that are misoriented.

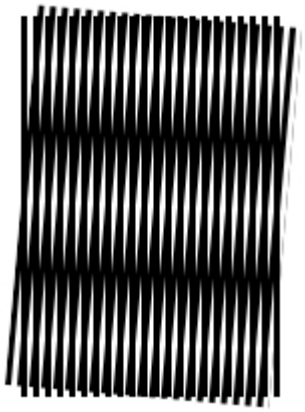

The top die was then gently prodded by hand in such a manner as to align the dies. Such a process would seem too inaccurate to produce the desired lateral registration of the 25 μm lines yet we repeatedly obtained excellent registration, such as that shown in Figure 9. This alignment accuracy was better than 1 μm, which is far better than the 5 μm accuracy of commercial aligners.

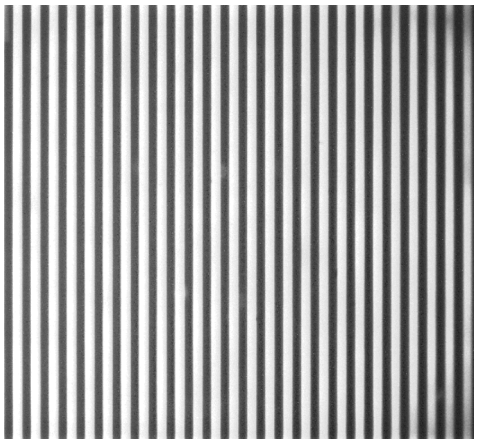

Figure 9. Essentially perfect alignment of two 2 cm square Pyrex die patterned with 25 μm Au lines spaced on 50 μm centers. This alignment was achieved manually, and is due to the surface interactions between the Au lines.

When these patterned die are placed together such that the lines are on the outer surfaces and the Pyrex surfaces are in contact, it is not possible to manually prod the upper die to achieve line alignment, which demonstrates the effectiveness of the interactions between the patterned surfaces. Alignment experiments were done with Au lines coated with dodecanethiol SAMs. On average, these die could be brought into alignment in less than half the time as for the uncoated lines. The ligand interfacial energy is minimized when the lines on the die are brought into registration, due to favorable interactions between the complementary ligand tails. It is interesting to note that partial alignment did not generally occur: Anytime a misorientation of the die was corrected by prodding the upper die at one corner it was found that the lines were automatically brought into lateral registration, allowing imaging through the die, such as in Figure 10.

Figure 10. (left) The left-hand side of this image is covered by the die pair patterned with Au lines and brought into registration by the interactions between these lines, which were coated with self-assembled monolayers of dodecanethiol. (right) When the image is magnified, the registered lines can be clearly seen. This image includes the upper right 'shoulder' of the thunderbird.

Bonding

Previous studies have reported that the temperature needed to form Au-Au bonds can be reduced if the Au surfaces are coated with alkanethiol SAMs (8,9). We have also found this to be the case for our SAM-coated ENIG/ENEPIG arrays, which formed strong bonds at 185^{o}C, with shear strengths of ~1.5 kg. The Argon plasma cleaned arrays did not bond at this temperature. We note that our experiments demonstrated bonding of Au pad arrays, whereas other studies typically bond arrays of Au bumps to blanket Au films on substrates.

The Au stud bumps formed strong bonds at 150-155°C, whether they were SAM-coated or Argon plasma cleaned. However, the SAM-coated Au bonds had a higher average shear strength (1.45 kg) and less deviation from the average than the Argon plasma cleaned Au bonds, whose average shear strength was 1.2 kg.

Conclusions

This study demonstrates the feasibility of utilizing the interactions between micropatterned, self-aligning surfaces that can vastly increase the alignment accuracy. We have computed the alignment forces and torque between two featured surfaces to illustrate how best to pattern surfaces to maximize the tendency to align. We have shown that a 2-d array of gold lines, whose width is half the periodicity, patterned onto Pyrex substrates leads to high resolution registration, enabling alignment accuracies far better than our aligners. An array of lines with a sinusoidal modulation in their spacing is a pattern that could greatly reduce the need for precision placement, while still retaining the high registration force given by the fine periodic line arrays. We have studied more complex patterns such as rectilinear pad assemblies, concentric rings, and spirals that point the way towards extremely precise alignment. Dodecanethiol self-assembled monolayers (SAMs) on the Au lines enhance the surface interactions, enabling registration in less time as for the uncoated lines.

After alignment is achieved, standard bonding techniques can be used to create precision permanent bonds. We have demonstrated Au-Au bonding of dodecanethiol SAM-coated Au features at 150-185°C. The SAM-coated and Ar-plasma treated Au stud bump arrays formed strong bonds at 150-155^{o}C. The ENIG/ENEPIG pad arrays with 100 nm Au films bonded only when SAM-coated and at 185^{o}C. The Argon plasma cleaned arrays did not bond at this temperature.

Acknowledgments

Sandia is a multiprogram laboratory operated by Sandia Corporation, a Lockheed-Martin Company, for the United States Department of Energy under Contract No. DE-AC04-94AL85000. This work was funded by Sandia's Laboratory Directed Research and Development program. We would like to thank Catalina Ahlers, Terri Romanic, Ben Thurston, Sharon Benson-Lucero, and Javier Gallegos for their contributions.

References

1. U. Srinivasan, D. Liepmann, R.T. Howe, *J. Microelectromech. Sys*., **10** [1], 17-24 (2001).
2. B.R. Martin, D.C. Furnange, T.N. Jackson, T.E. Mallouk, T.S. Mayer, *Adv. Funct. Mater.*, **11** [5], 381-386 (2001).
3. X. Xiong, Y. Hanein, J. Fang, Y. Wang, W. Wang, D.T. Schwartz, K.F. Bohringer, *J. Microelectromech. Sys*., **12** [2], 117-127 (2003).
4. M.R. Tupek, K.T. Turner, *J. Vac. Sci. Technol. B*., **25** [6], 1976-1981 (2007).
5. J. Dalin, J. Wilde, A. Zulfiqar, P. Lazarou, A. Synodinos, N. Aspragathos, *Microelectronic Engineering*, **87**, 159-162 (2010).
6. T. Fukushima, E. Iwata, T. Konno, J.-C. Bea, K.-W. Lee, T. Tanaka, M. Koyanagi, *Appl. Phys. Lett*., **96**, 154105(1-3) (2010).
7. A.H. Slocum, A.C. Weber, **12** [6], 826-834 (2003).
8. X.F. Ang, F.Y. Li, W.L. Tan, Z. Chen, C.C. Wong, *Appl. Phys. Lett.*, **91**, 061913(1)-061913(3) (2007).
9. L.C. Chin, X.F. Ang, J. Wei, Z. Chen, C.C. Wong, *Thin Solid Films*, **504**, 367-370 (2006).